Influence of Short Fiber Encapsulated in Hybrid Hydrogel For 3d Bioprinting Process: Aspect of Rheological Properties

Abstract ID: 2274

Slesha Tuladhar, Scott Clark, and MD Ahasan Habib*

Sustainable Product Design and Architecture Department, Keene State College, Keene, NH 03435, USA.

Abstract

Extrusion-based three-dimensional (3D) bio-printing is one of the several 3D bioprinting methods that is frequently used in current times. This method enables the accurate deposition of cell-laden bio-ink while ensuring a predetermined scaffold architecture that may allow living tissue regeneration. Natural hydrogels are a strong choice for bio-ink formulation for the extrusion-based 3D bioprinting method because they have a combination of unique properties, which include biocompatibility, reduced cell toxicity, and high-water content. However, due to its low mechanical integrity, hydrogel frequently struggles to retain structural stability. To overcome this challenge, we evaluated the rheological characteristics of distinct hybrid hydrogels composed of carboxymethyl cellulose (CMC), a widely used alginate, and nanofibers generated from cellulose (TEMPO-mediated nano-fibrillated cellulose, TONFC). Therefore, to examine the rheological properties, a set of compositions was developed incorporating CMC (1%–4%), alginate (1%–4%), and higher and lower contents of TONFC (0.5%) and (0.005%) respectively. From the flow diagram, the shear thinning coefficients of n and K were calculated, which were later linked to the 3D printability. With the guidance of diverse nanofiber ratios, it is possible to regulate the rheological properties and create 3D bio-printed scaffolds with well-defined scaffold architecture.

Keywords

3D bioprinting, Rheology, Shear Thinning, Printability.

1. Introduction

Among various processes in tissue engineering and regenerative medicine fields for generating tissue and organ-like structures, Additive Manufacturing (AM), commonly known as 3D Bioprinting, is a powerful technology [1, 2]. Extrusion-based bioprinting has become popular due to being easy to control, allowing a wide range of materials, and having a high concentration of cells [3, 4]. This unique technique helps fabricate a temporary structure, typically known as a scaffold, composed of biomaterials, living cells, and a cell-supporting growth medium [5]. The performance of this biologically functional scaffold depends on the capacity to maintain structural integrity and support cell survivability during and after the bioprinting process [6]. Selecting a proper biomaterial can equally support maintaining the scaffold's structural integrity and cell viability by creating a cell-friendly environment, i.e., Extra Cellular Matrix (ECM) [7, 8]. While the positive impact of natural hydrogels on producing ECM environment has widely been reported, it demands more research to ensure the structural integrity of the fabricated scaffolds [9]. Researchers have been mixing multiple biomaterials to prepare hybrid hydrogels to overcome this challenge, ensuring suitable rheological properties to maintain defined structural integrity without compromising cell survivability [10]. Easy processing techniques and the capability to regulate the rheological behavior make sodium alginate one of the first hydrogel choices for the extrusion-based bioprinting process [11]. Carboxymethyl cellulose (CMC) is another polysaccharide and cellulose derivative that changes viscosity [12]. The binding of the CMC's matrix protein aids cell adhesion and movement [13]. In recent times, nano-scale reinforcements such as polylactic acid (PLA) nanofibers and nano-fibrillated cellulose (NFC) have been utilized to enhance the mechanical and biological (for example, cell development) capabilities of the base hydrogel material [14, 15]. The surface of the NFC-based gel is altered by oxidation using 2,2,6,6 tetramethyl-1-piperidinyloxy (TEMPO) to add negatively charged carboxylate ions, known as TO-NFC, to improve uniformity, dispersibility, homogeneity, and printability (TempO-NFC). Even higher zero-shear viscosity (without applying pressure) of any hydrogel can help maintain the scaffold's structural integrity. This may jam the dispensing nozzle, requiring additional force to clear it, distorting the print, and lowering cell viability [16]. This scenario establishes a constraint to use every component of a hybrid hydrogel up to a certain amount.

In our earlier research, we proposed a bio-ink with alginate, carboxymethyl cellulose (CMC), and TEMPO-mediated nano-fibrillated cellulose-TONFC for the first time limiting the solid content 5% (2% alginate, 2% CMC, and 1% TONFC). That bio-ink ensured fabrication of scaffold with a build height of 9.6mm and 93% cell viability [17]. As an extension of that work, we studied the effect of very low and high percentage of TO-NFC in this paper. Extensive rheological experiments were conducted on a set of compositions prepared with a varying percentage of alginate, CMC, and TO-NFC. Flow behavior of those compositions was studied and co-related with various percentages of TO-NFC. Finally, we chose some compositions having very low and high percentages of TO-NFC to 3D print filament, analyze the shape fidelity, and co-relate the result.

2. Materials and Methods

2.1 Processing of TO-NFC

The Process Development Center (PDC) at the University of Maine provided dry TEMPO nano-fibrillated cellulose (TO-NFC) $[(C_6H_{10}O_5)_x(C_6H_9O_4CO_2Na)_y]$ with a carboxylate level ranging from 0.2 to 2 mmol/g solids. A magnetic stand-up stirrer set at 600 revolutions per minute was used to prepare two various amounts of dry TO-NFC, such as 0.005% and 0.5%, for 24 hours at room temperature.

2.2 Hybrid Hydrogel Preparation

A magnetic stand-up stirrer was used to combine produced TO-NFC using section 2.1 with varying amounts of medium (viscosity 2000 cps of 2% in water) viscous Alginate (1, 2, 3, and 4%, w/v) and CMC (1, 2, 3, and 4%, w/v) (pH: 6.80) from Sigma-Aldrich, St. Louis, MO, USA. Table 1 contains the materials that were employed in this study to make the bio-ink, and the letters "A," "C," and "T" stand for Alginate, Carboxymethyl cellulose, and Tempomediated nano fibrillated cellulose, respectively. The weight % of the component blended with the water to create the material compositions is indicated by the numerical subscripts. The inclusion of CMC and TO-NFC will raise the material's overall viscosity, which may help with better shape fidelity [25, 33].

Table 1: Various compositions prepared with different weight percentages of alginate (1, 2, 3, and 4%, w/v), CMC (1, 2, 3, and 4%, w/v), and TO-NFC (0.005% and 0.5%, w/v).

Alginate	CMC	TO-NFC	Symbol	TO-NFC	Symbol
(A), %	(C), %	(T), %		(T), %	
1	1		$A_1C_1T_{0.005}$		$A_1C_1T_{0.5}$
	2		$A_1C_2T_{0.005}$		$A_1C_2T_{0.5}$
	3		$A_1C_3T_{0.005}$		$A_1C_3T_{0.5}$
	4		$A_1C_4T_{0.005}$		$A_1C_4T_{0.5}$
2	1		$A_2C_1T_{0.005}$		$A_2C_1T_{0.5}$
	2		$A_2C_2T_{0.005}$		$A_2C_2T_{0.5}$
	3	0.005	$A_2C_3T_{0.005}$	0.5	$A_2C_3T_{0.5}$
	4		$A_2C_4T_{0.5}$		$A_2C_4T_{0.5}$
3	1		$A_3C_1T_{0.005}$		$A_3C_1T_{0.5}$
	2		$A_3C_2T_{0.005}$		$A_3C_2T_{0.5}$
	3		$A_3C_3T_{0.005}$		$A_3C_3T_{0.5}$
4	1		$A_4C_1T_{0.005}$		$A_4C_1T_{0.5}$
	2		$A_4C_2T_{0.005}$		$A_4C_2T_{0.5}$

2.3 Flow behavior of hybrid hydrogels

We performed the rheological tests, specifically the flow behavior of hybrid hydrogels using a rotational rheometer (25.0 mm flat plate, MCR 102 from Anton Paar in Graz, Austria) with parallel plate geometry. All data were collected at room temperature (25°C) with the goal of performing the extrusion operation there to have a rapid gelation of the deposited filament [18]. The plate-to-plate spacing was kept at 1.0 mm. We mainly concentrated on the compositions' flow behavior. A steady rate sweep test with a varied shear strain ranging from 0.1 to 100 s⁻¹ was undertaken for flow curve analysis. The Power-Law Equation (Equation 1) was fitted to the curves obtained from shear strain rate vs viscosity [19] to analyze the shear-thinning behavior of the hybrid hydrogels. Next, the shear thinning co-efficient of n and K were calculated by fitting a curve to the following equation:

$$\eta = K\dot{\gamma}^{\text{n-1}} \tag{1}$$

Where the viscosity is η and the shear rate is $\dot{\gamma}$. Shear stress develops throughout the material when it is extruded through the nozzle and is greater along the nozzle wall. The viscosity vs shear rate data for each hybrid hydrogels were fitted using the nonlinear curve fitting module (Allometric) of OriginPro 2022b (Originlab, Northampton, MA, USA) to calculate the values of n and K.

2.4 3D printing and shape fidelity analysis

The scaffolds and filaments were created using a 3D bio-printer that uses extrusion called BioX (CELLINK, Boston, MA). Accordingly, we synthesized hybrid hydrogels, put them in a 3.0 ml disposable nozzle, and pneumatically extruded them onto a fixed build plane. The printing parameters we employed to create the scaffolds included an air pressure range of 80–170 kPa, a nozzle diameter of 450 m, and a print speed of 8 mm/s. Rhino 6.0 (https://www.rhino3d.com), a visual basic-based CAD program, was used to create and specify the vectorized toolpath of a scaffold. A Bio-X compliant file containing the toolpath coordinates and all process parameters was created using Slicer (https://www.slicer.org), a G-code generation program, to build the scaffold. We followed a layer-upon-layer fashion to deposit the materials. A brightfield CK Olympus microscope was used to capture the images of fabricated filaments [20]. The width of the filament is determined using ImageJ software.

2.5 Statistical analysis

We collected data following a format of "mean \pm standard deviation" and analyzed them using a significance level of p = 0.05 with a two-way ANOVA. Calculations were done with n=3 unless otherwise stated. We used a statistical software, Origin Pro 2022b (OriginLab, Northampton, MA) to analyze quantitatively and graphically.

3. Results and discussions

The shear thinning behavior of the compositions was examined by the Flow Curve test on all of the hybrid hydrogels. This demonstrated the effects of varying Nano fiber concentrations on the viscosities of various compositions, as shown in the figures below:

3.1 Flow behavior of hybrid hydrogels

All hybrid hydrogels with various concentrations of Alginate and CMC displayed a shear thinning behavior with the addition of 0.005% TO-NFC. The viscosity of $A_1C_1T_{0.005}$ was the lowest, but $A_1C_4T_{0.005}$ and $A_2C_4T_{0.005}$ had the greatest and most comparable viscosities. Figures 1 displays the results. Similar to this, $A_1C_1T_{0.5}$ has the lowest viscosity spectrum, whereas $A_1C_4T_{0.5}$ has the greatest. Additionally, compositions containing 0.5% TO-NFC have higher viscosities than compositions containing 0.005% TO-NFC, when the two are compared. This means that, while the composition of Alginate and CMC is held constant, the higher the concentration of the TO-NFC, the higher the viscosity of the composition.

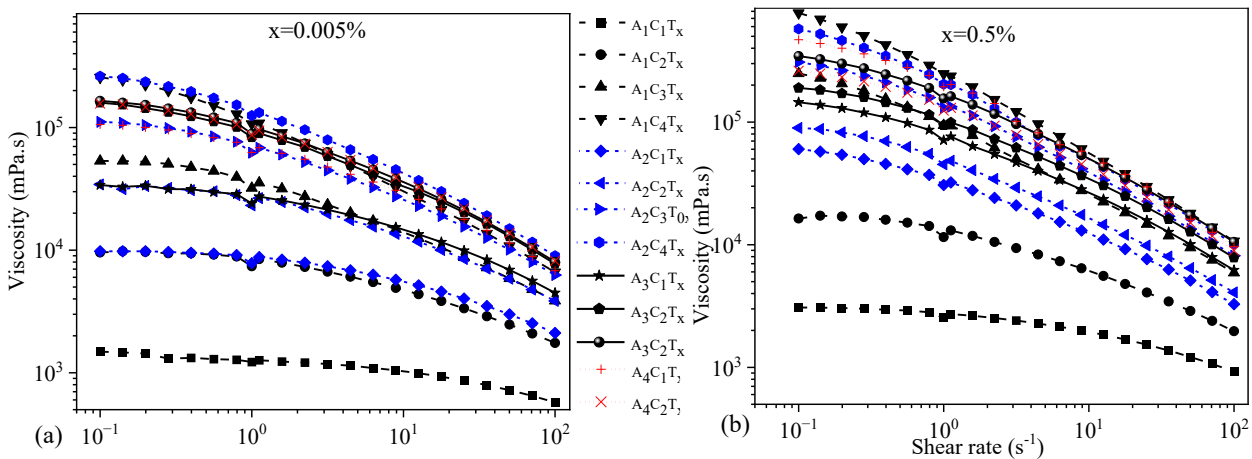


Figure 1: Viscosities of hybrid hydrogels with respect to shear rate for (a)0.005% TO-NFC and (b) 0.5% TO-NFC

As noted in section 2.2, the values of n and K were calculated by fitting the viscosity vs. shear rate data for each composition using a nonlinear curve fitting module (Allometric). A satisfactory match is indicated when the adjusted R-square value for each composition is more than 90%. Figure 2 illustrates the fit curves that were used to calculate the n and K values for $A_1C_4T_{0.005}$ and $A_1C_4T_{0.5}$, respectively. According to Figure 2, the adjusted R-square values for the curves fitted for the for $A_1C_4T_{0.005}$ and $A_1C_4T_{0.5}$ compositions were 98% and 99%, respectively. The n and K values for every other composition were also established in this study. When the shear thinning factors, n and k, of the compositions depicted in Figure 3 are calculated.

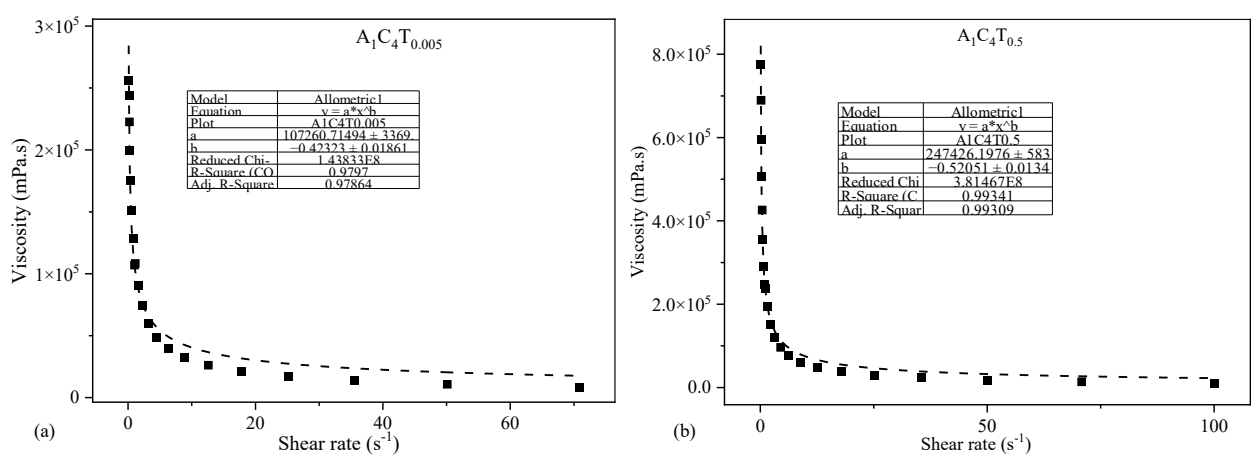


Figure 2: Estimating the values of shear thinning factors (n and K) of compositions (a) $A_1C_4T_{0.005}$ and (b) $A_1C_4T_{0.5}$. For $A_1C_4T_{0.005}$, n and K values were 0.58 and 107260 ± 3369 (mPa.s) with an R-square value of 0.98, whereas, for $A_1C_4T_{0.5}$, n and K values were 0.48 and 247426 ± 5839 (mPa.s) with an R-square value of 0.99.

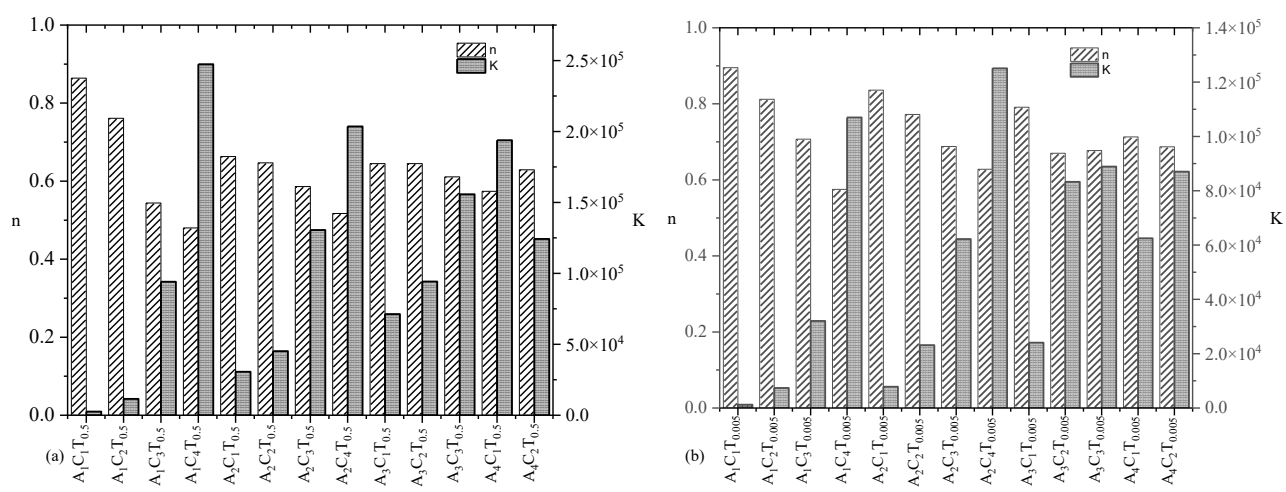


Figure 3: Shear thinning factors (n and K) of compositions composed with various percentages of alginate (1-4%) and CMC (1-4%) with a constant percentage (a) 0.5% and (b) 0.005% of TO-NFC. All n values less than 1 confirm a shear-thinning behavior of all compositions.

Figure 4 also shows an intriguing phenomenon where the n and K values had an inverse relationship regardless of the TO-NFC percentage (either 0.005% or 0.5%). The hydrogel has the same viscosity as water if the value of n is near to 1.0. A lower n value indicates a greater potential for shear thinning (i.e., tendency of higher viscosity reduction with small increment of the shear rate on the hydrogel). As shown in Figure 3, the n values for $A_1C_1T_{0.005}$ and $A_1C_1T_{0.5}$, respectively, are 0.90 and 0.86, whereas the K values are 1222 and 2535 mPa.s. The n and K values are inversely related for both compositions. $A_1C_1T_{0.5}$ is more viscous than $A_1C_1T_{0.005}$, according to either the n or K values.

At the shear rate of 1.0 s^{-1} , the shear thinning factor K is calculated. Throughout the study, we will mostly use the K value for comparison purposes. The viscosity was determined by the proportion of CMC with a constant percentage of TO-NFC (either 0.005% or 0.5%) and alginate (either 1%, or 2%, or 3%, or 4%). As an illustration, $A_1C_4T_{0.005}$ had the highest K value among $A_1C_1T_{0.005}$, $A_1C_2T_{0.005}$, $A_1C_3T_{0.005}$, and $A_1C_4T_{0.005}$. Figure 1 illustrates a similar phenomenon that was seen for $A_2C_4T_{0.005}$, $A_3C_3T_{0.005}$, and $A_4C_2T_{0.005}$. However, CMC could not always be under control of the K value for a similar percentage of solid content (i.e., summation of percentages of all components into a particular composition). As an illustration, the K values for the following compounds were 106999, 62205, 83266, and 62491 mPa.s, respectively: $A_1C_4T_{0.005}$, $A_2C_3T_{0.005}$, $A_3C_2T_{0.005}$, and $A_4C_1T_{0.005}$. The total solid content for each composition in this case is 5.005%. With a 4% CMC, composition ($A_1C_4T_{0.005}$) displayed the greatest K value. It is evident from the statistics that there was no pattern between the K value and the CMC percentage. A similar pattern was also seen for the K values of $A_1C_4T_{0.5}$, $A_2C_3T_{0.5}$, $A_3C_2T_{0.5}$, and $A_4C_1T_{0.5}$ (247426, 130574, 94258, and 193857 mPa.s, respectively)

as shown in Figure 2. This remained true even when the fraction of TO-NFC was increased from 0.005% to 0.5%. Here, the total solid content for each composition is 5.5%, and the proportion of CMC did not entirely determine K value.

3.2 Filament width after 3D printing

To analyze the effect of TO-NFC on the printability of various compositions having 0.005% and 0.5% TO-NFC were considered to 3D print. Total eight compositions such as $A_1C_4T_{0.005}$, $A_1C_4T_{0.05}$, $A_4C_1T_{0.005}$, and $A_4C_1T_{0.5}$, were chosen to print them with three different print speeds such as 5, 10, and 15 mm/s as shown in Figure 4. Our first observation was all compositions were 3D-printable and filaments preserved the shape. Filaments fabricated with higher CMC with similar A and TO-NFC showed larger width. Therefore, irrespective of print speed, filaments fabricated with $A_4C_1T_{0.005}$, and $A_4C_1T_{0.005}$ showed 35% larger width with respect to the filament fabricated with $A_1C_4T_{0.5}$, and $A_4C_1T_{0.005}$ showed 21%, 28%, and 29% larger width with respect to the filament fabricated with $A_1C_4T_{0.005}$ and $A_1C_4T_{0.005}$ at 5, 10, and 15 mm/s print speed, respectively as shown in Figure 4

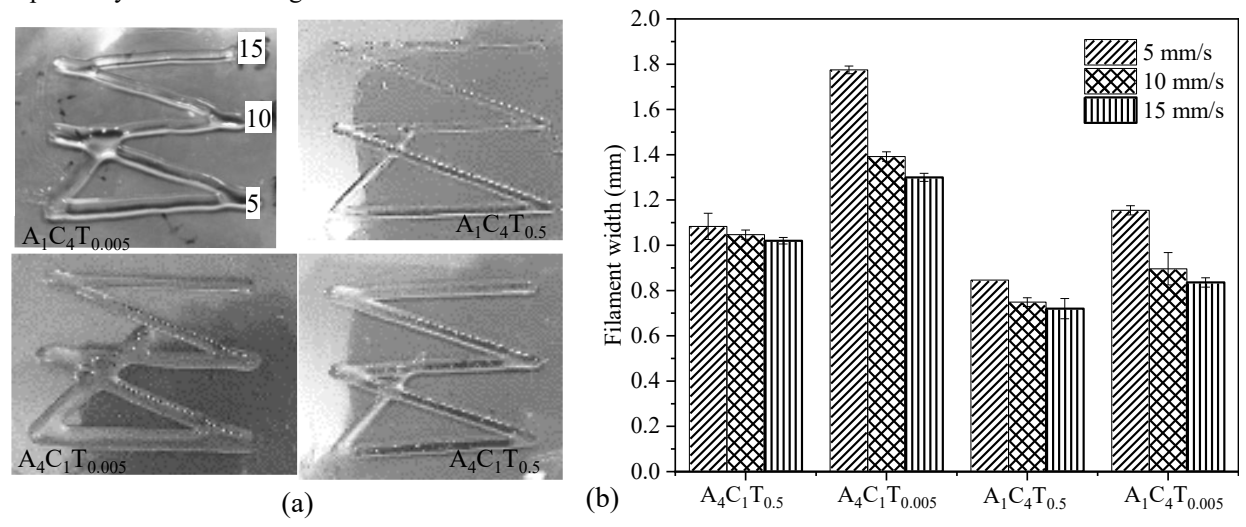


Figure 4: Shear thinning factors (n and K) of compositions composed with various percentages of alginate (1 and 4%) and CMC (1 and 4%) with a constant percentage (a) 0.5% and 0.005% of TO-NFC. All n values less than 1 confirm a shear-thinning behavior of all compositions.

4. Conclusion

Rheological analysis was done in this study for a total of 23 compositions to determine the impact of different TO-NFC percentages on different alginate and CMC percentages. This experimental analysis can assist in identifying the proper material to achieve geometrical fidelity by managing the filament width while fabricating a large-scale functional tissue scaffold with the appropriate hybrid hydrogel. In the future, we will print filaments with all compositions, measure the filament's width, and investigate an analytical model that can relate the ratio of TO-NFC to the filament's width. The 3D bio-fabrication of the customized anisotropic scaffolds can be guided by the depicted characterization procedures, which will help with the creation of functional tissue in the future.

Acknowledgements

Research was supported by New Hampshire-EPSCoR through BioMade Award #1757371 from National Science Foundation and New Hampshire-INBRE through an Institutional Development Award (IDeA), P20GM103506, from the National Institute of General Medical Sciences of the NIH.

References

- [1] M. Alonzo, S. AnilKumar, B. Roman, N. Tasnim, and B. Joddar, "3D Bioprinting of cardiac tissue and cardiac stem cell therapy," *Translational Research*, 2019.
- [2] Y. Chen *et al.*, "3D Bioprinting of shear-thinning hybrid bioinks with excellent bioactivity derived from gellan/alginate and thixotropic magnesium phosphate-based gels," *Journal of Materials Chemistry B*, 2020.

- [3] J. H. Chung *et al.*, "Bio-ink properties and printability for extrusion printing living cells," *Biomaterials Science*, vol. 1, no. 7, pp. 763-773, 2013.
- [4] Z. M. Jessop *et al.*, "Printability of pulp derived crystal, fibril and blend nanocellulose-alginate bioinks for extrusion 3D bioprinting," *Biofabrication*, vol. 11, no. 4, p. 045006, 2019/07/08 2019, doi: 10.1088/1758-5090/ab0631.
- [5] Z. Yazdanpanah, J. D. Johnston, D. M. Cooper, and X. Chen, "3D bioprinted scaffolds for bone tissue engineering: state-of-the-art and emerging technologies," *Frontiers in Bioengineering and Biotechnology*, vol. 10, 2022.
- [6] A. Schwab, R. Levato, M. D'Este, S. Piluso, D. Eglin, and J. Malda, "Printability and shape fidelity of bioinks in 3D bioprinting," *Chemical reviews*, vol. 120, no. 19, pp. 11028-11055, 2020.
- [7] S. J. Bryant and K. S. Anseth, "Hydrogel properties influence ECM production by chondrocytes photoencapsulated in poly (ethylene glycol) hydrogels," *Journal of Biomedical Materials Research: An Official Journal of The Society for Biomaterials and The Japanese Society for Biomaterials*, vol. 59, no. 1, pp. 63-72, 2002.
- [8] M. Costantini *et al.*, "3D bioprinting of BM-MSCs-loaded ECM biomimetic hydrogels for in vitro neocartilage formation," *Biofabrication*, vol. 8, no. 3, p. 035002, 2016.
- [9] T. H. Jovic, G. Kungwengwe, A. C. Mills, and I. S. Whitaker, "Plant-Derived Biomaterials: A Review of 3D Bioprinting and Biomedical Applications," *Frontiers in Mechanical Engineering*, 10.3389/fmech.2019.00019 vol. 5, p. 19, 2019.
- [10] B. Duan, L. A. Hockaday, K. H. Kang, and J. T. Butcher, "3D bioprinting of heterogeneous aortic valve conduits with alginate/gelatin hydrogels," *Journal of biomedical materials research Part A*, vol. 101, no. 5, pp. 1255-1264, 2013.
- [11] M. Di Giuseppe *et al.*, "Mechanical behaviour of alginate-gelatin hydrogels for 3D bioprinting," *Journal of the mechanical behavior of biomedical materials*, vol. 79, pp. 150-157, 2018.
- [12] T. Agarwal, S. G. H. Narayana, K. Pal, K. Pramanik, S. Giri, and I. Banerjee, "Calcium alginate-carboxymethyl cellulose beads for colon-targeted drug delivery," *International journal of biological macromolecules*, vol. 75, pp. 409-417, 2015.
- [13] Q. Garrett *et al.*, "Carboxymethylcellulose binds to human corneal epithelial cells and is a modulator of corneal epithelial wound healing," *Investigative ophthalmology & visual science*, vol. 48, no. 4, pp. 1559-1567, 2007.
- [14] L. K. Narayanan, P. Huebner, M. B. Fisher, J. T. Spang, B. Starly, and R. A. Shirwaiker, "3D-bioprinting of polylactic acid (PLA) nanofiber—alginate hydrogel bioink containing human adipose-derived stem cells," *ACS Biomaterials Science & Engineering*, vol. 2, no. 10, pp. 1732-1742, 2016.
- [15] D. Nguyen *et al.*, "Cartilage tissue engineering by the 3D bioprinting of iPS cells in a nanocellulose/alginate bioink," *Scientific reports*, vol. 7, no. 1, p. 658, 2017.
- [16] H.-J. Kong, K. Y. Lee, and D. J. Mooney, "Decoupling the dependence of rheological/mechanical properties of hydrogels from solids concentration," *Polymer*, vol. 43, no. 23, pp. 6239-6246, 2002.
- [17] M. Habib and B. Khoda, "Fiber Filled Hybrid Hydrogel for Bio-Manufacturing," *Journal of Manufacturing Science and Engineering*, pp. 1-38, 2020.
- [18] L. Ouyang, R. Yao, Y. Zhao, and W. Sun, "Effect of bioink properties on printability and cell viability for 3D bioplotting of embryonic stem cells," *Biofabrication*, vol. 8, no. 3, p. 035020, 2016.
- [19] D. Therriault, S. R. White, and J. A. Lewis, "Rheological behavior of fugitive organic inks for direct-write assembly," *Applied Rheology*, vol. 17, no. 1, pp. 10112-1-10112-8, 2007.
- [20] R. S. Kumar V, Cutkosky M, Dutta D, "Representation and processing heterogeneous objects for solid freeform fabrication," ed. Sixth IFIP WG 5.2 International Workshop on Geometric Modelling: Fundamentals and Applications, Tokyo, Japan, The University of Tokyo, 1998.